Phosphorylated xanthan gum-Ag(I) complex as antibacterial viscosity enhancer for eye drops formulation

Phosphorylated Xanthan Gum-Ag(I) complex as antibacterial viscosity enhancer for eye drops formulation

Gemma Leone[#1, 2], Simone Pepi[1], Marco Consumi[1, 2], Fariba Fahmideh Mahdizadeh[1], Stefania Lamponi[1, 2], Agnese Magnani[#1, 2]

[1]Department of Biotechnology, Chemistry and Pharmacy, University of Siena, via A. Moro 2, Siena 53100, Italy

[2] INSTM, via G. Giusti 9, 50121 Firenze, Italy

#corresponding authors: Gemma Leone: gemma.leone@unisi.it; +39-0577-232109; Agnese Magnani: agnese.magnani@unisi.it; +39-0577-232108.

Abstract

Topical instillation of eye drops represents the treatment of choice for many ocular diseases. Ophthalmic formulations must meet general requirements, i.e. pH, osmolality, transparency and viscosity to ensure adequate retention without inducing irritation and the development of eye infections. We developed a phosphorylated xanthan gum–Ag(I) complex (XGP-Ag) showing pH (pH= 7.1± 0.3) and osmolality values (311± 2 mOsm/kg) close to that of human tears (pH = 6.5–7.6 and 304 ± 23 mOsm/kg) thanks to the presence of phosphate moieties along the chain. The presence of phosphate groups covalently bound to the XG chains avoids their dispersion in fluid, thus reducing the risk of corneal calcification. 0.02% w/v XGP-Ag solution showed high transparency (higher than 95% along the entire visible range), adequate refractive index (1.334±0.001) and viscosity in the range: γ $1s^{-1}$-$10000\,s^{-1}$ (26.4±0.8 - 2.1±0.4 mPa·s). Its cytotoxicity and capability to hinder bacterial proliferation was also verified.

Keywords: Xanthan Gum; Silver ions; antibacterial; eye drops; viscosity

1. Introduction

Eye is a very complex organ exhibiting several protective barriers. The dynamic lachrymal system and the small volume that the lower conjunctival sac can accommodate (i.e. 30 μL) contribute to the very low ocular bioavailability for any drug. Indeed, less than 5% of substances administered by eye drops can reach the action site (Račić, Čalija, Milić, Milašinović & Krajišnik, 2019). Improved efficiency of eye drops is based on increasing their residence time on ocular surface, using viscosity enhancers, mainly high molecular weight hydrophilic polymers (Imperiale, Acosta & Sosnik, 2018; Jumelle, Gholizadeh, Nasim, Annabi & Dana, 2020). A wide range of natural, synthetic or semisynthetic polymers complies with the requirement of viscosity enhancers. Carbomers (Said dos Santos et al, 2020), hyaluronic acid (Cappelli et al, 2016; Salzillo et al, 2016), polyvinyl alcohol (Piluso, Sudre, Boisson-Da Cruz, Bounor-Legaré & Espuche, 2018) cellulose derivatives (Karakus et al, 2020) and gellun gum (Leone et al, 2020) have been extensively studied and used. Among them, polysaccharides, thanks to the formation of macromolecular ionic complexes with bioactive substances, can improved the bioavailability of administered drugs lengthening their therapeutic effect. In particular, anionic and cationic polymers show a better mucoadhesive capacity in comparison to non-ionic ones (Ludwig, 2005). Xanthan gum (XG), an anionic exopolysaccharide secreted by the bacterial plant pathogen Xanthomonas, is widely used in controlled drug release and cosmetics, because of its low toxicity and high stability in a wide range of temperatures and pH (Dzionek et al, 2021). XG itself can also be used as active specie since it is able to promote the corneal epithelial tissue regeneration, once coupled with HA (Rinaudo, 2008). Beside the viscosity and bioavailability, eye drop preparations require special attention to sterility, preservation, isotonicity and buffering (Wroblewska, Kucinska, Murias, & Lulek, 2015). Quite all the formulations contain benzalkonium chloride (BAC), a quaternary ammonium salt commonly used

in eye drops for its microbicidal properties. BAC hinders microbial proliferation before and after instillation. Indeed, owing to its vascularization most of the drug that enters the conjunctiva is absorbed into the systemic circulation. Moreover, frequent administrations are necessary due to the very low bioavailability of instilled drugs, thus increasing the risk of infection (Jumelle et al, 2020). Nevertheless, BAC is known to favor the onset of dry eye disease (DED) (Zhang et al, 2020). The addition of Ag(I) could represent an alternative. Silver ions are largely used in ointments and wound dressing because of their non-specific biocidal action against a broad spectrum of bacteria, including several antibiotic resistant strains and fungal species. Even if silver ions show an effective antimicrobial action, they may induce dose-related toxicity in tissue when their release is not controlled (Agarwal, et al, 2010). However, Ag(I) ions are more toxic for procaryotes then for mammalian cells, so, tuning properly the release of metal ions, they can act as antibacterial agent without harm the mammalian tissues and cells (Greulich et al, 2012). Indeed, silver is one of the unique metals that behaves specifically versus microorganisms, thanks to its ability to bind to microbial proteins, causing changes in the structure of the cell walls and membranes of the bacteria (Bonilla-Gameros, Chevallier, Sarkissian & Mantovani, 2020; Waszczykowska, Żyro, Jurowski & Ochocki, 2020).

We conjecture that the use of phosphorylated xanthan gum polymer able to strictly coordinate silver ions can be used to gain both adequate viscosity and antimicrobial properties, two fundamental requirements for effective eye drops. In this regards, phosphorylation should also guarantee an appropriate osmolality and pH buffering capacity avoiding the use of free phosphate moieties that could induce corneal calcification.

2. Experimentals

2.1 Materials

Xanthan Gum (XG) (MW 10 MDa), Sodium trimethaphosphate (STMP), Ag standard for AAS, cellulose dialysis membrane (MWCO 12-14 KDa) and all the other reagents were purchased from Sigma-Aldrich. Specroquant® spectrophotometric kit for the phosphate assay was purchased from Merck. All solutions and materials used for cell cultures were provided by Lonza (Belgium). American Type Culture Collection (USA) and Invitrogen (USA) supplied, respectively, mouse immortalized fibroblasts NIH3T3 and primary adult human endothelial cells (HMVEC).

2.2 Xanthan Gum phosphorylation (XGP)

1% w/v solution of XG was prepared solubilizing the polysaccharide in bi-distilled water at room temperature, under magnetic stirring. The solution was basified to pH 12 with NaOH 2M. The phosphorylating agent trisodium trimetaphosphate (STMP) was then added in a molar ratio STMP: XG 10: 1. After 2 h the reaction solution was neutralized by adding HCl (2M). The product was purified by dialysis, using a cellulose membrane (MWCO 12-14000 Da), checking the conductivity (GLP32 CRISON) of the washing solutions till complete elimination of the unreacted STMP. Aliquots (2 mL) of washing solutions were dried on IR crystal (Nicolet Thermo 5700 spectrometer) and infrared spectra recorded to further confirm the absence of unreacted STMP. The purified product (XGP) was then lyophilized (5Pascal, LIO5P-4K).

The phosphorylation degree was determined by spectrophotometry, using a UV-VIS Lambda 25 (PerkinElmer Instruments). A commercial kit (Test Spectroquant Merck KqaAe Darmstadt e Germany e ISO6878/1 and US-standard Methods 4500-P-E) was used following the producer instruction. Briefly, the sample at solid state was calcinated and solubilized in bidistilled water to obtain 0.1% w/v solution. The absorbance of the resulting solution was measured at a wavelength of 713 nm. Calibration curve was constructed using five non zero points in the range of 0.5 mg/L- 10 mg/L ($R^2 = 0.9999$). The phosphorylation degree was expressed as % P (Leone et al, 2019 a).

2.3 Complex formation (XGP-Ag)

Established amount of dried polymer was solubilized in 10^{-3} M $AgNO_3$ solution, protected from direct exposure to light. After 24 h, the obtained polymer solution (0.4% w/v) was dialyzed against bidistilled water, to remove silver ions. The washing process was continued until no detectable metal ion concentration was revealed. The purification process was verified by measuring the conductivity of the washing water using a CRISON GLP32 conductivity meter. Finally, the product was lyophilized (5Pascal, LIO5P-4K freeze dryer).

The Ag content of the sample XGP-Ag was determined by Atomic Absorption Spectroscopy (AAS) using a AAS - 220Z (Varian). The analysis was performed under Argon at a wavelength of 328 nm, with a thermal program consisting of different steps: from 120°C (evaporation of water), followed by steps to 400°C-600°C-900°C (pyrolysis), till 2000°C (atomization).

2.4 Infrared Analysis

FTIR spectra of native, phosphorylated and silver containing polymers were recorded between 4000 and 750 cm^{-1} using a Nicolet Thermo 5700 spectrometer equipped with an attenuated total reflection (ATR) accessory and a 45° Germanium crystal as internal reflection element. A Mercury–Cadmium–Tellurium (MCT) detector was used, purging the apparatus with nitrogen. 64 scans were averaged (resolution: 2.0 cm^{-1}). The frequency scale was internally calibrated with a helium–neon reference laser to an accuracy of 0.01 cm^{-1}. Baseline and spectra correction were performed using the OMNIC correction ATR software (Leone et al, 2019 b).

2.5 Thermogravimetric analysis (TGA)

STD Q600 analyzer (TA Instruments, Leatherhead, United Kingdom) was used to quantify polymers weight loss as a function of heating. 10–15 mg of dry polymers (XG, XGP and XGP-Ag) and a commercial eye gel drops (CegD) product (in dry state) were inserted in a platinum crucible and heated from RT to 800 °C (heating ramp 10 °C/min) under nitrogen flow (100 mL/min) (Leone et al, 2017). Results are expressed as mean value ± SD of three replicates.

2.6 Rheological Properties

The rheological analyses were performed at 37 °C with a Discovery Hybrid Rheometer – 2 (DHR-2, TA Instruments). XG, XGP and XGP-Ag solutions with a concentration range 0.02%-1% were analyzed after being filtered through a 0.22 µm filter. A 1° cone-plate stainless steel geometry (40 mm, truncation 28.0 µm) equipped with Peltier steel plate environmental system was used for the tests. Results are expressed as mean value of three replicates.

Viscosity was measured with a flow sweep test, in the range of shear rate ($\dot{\gamma}$) from 0.01 s^{-1} to 10 000 s^{-1}. A 0.1% -20% strain sweep test was run to find the linear viscoelastic region (LVR) for frequency 0.1 Hz, 1 Hz and 10 Hz. Then, G' and G" were measured in a frequency ramp from 0.1 Hz to 10 Hz with a 1% of strain, selected within the strain values in the LVR. All measurements were conducted also on the commercial formulation (CegD).

2.7 Transparency

0.02% w/v, 0.5% w/v and 1% w/v solutions of XGP-Ag after sterilization by filtration through 0.22 µm filter and the commercial formulation (CegD) were analyzed in terms of the percentage of transmittance (%T). Three scans from 700 to 380 nm were averaged using a UV–vis Spectrophotomer (Perkin Elmer Lamda 25; optical pathway, 10 mm; cuvettes, PMMA/UV grade) (Lin, Lin & Yang, 2009).

Refractive index values for XGP-Ag formulations and CegD were measured at room temperature using the refractometer (Atago refractometer, Japan) by placing one drop of the samples on the slide of the refractometer (Mahboobian, Mohammadi & Mansouri, 2020). Results are expressed as mean value ± SD of three replicates.

2.8 Biological tests

144 The *in vitro* cytotoxicity was evaluated following the direct contact test proposed in "ISO 10993-5
145 biological evaluation of medical devices – Part 5: tests for cytotoxicity: in vitro methods". This test
146 is suitable for samples with various shapes, sizes or physical states (i.e. liquid or solid). The test was
147 performed preparing the cell cultures and following the protocol as reported by Leone et al. (Leone
148 et al, 2019 c). Briefly, Mouse fibroblasts (NIH3T3), and primary adult human microvascular
149 endothelial cells (HMVEC) were used to test cytotoxicity. HMVEC were propagated in medium
150 131, NIH3T3 cell in DMEM. Both media were supplemented with 10% fetal calf serum, 1% l-
151 glutamine-penicillin–streptomycin solution and 1% non-essential amino acid solution and incubated
152 at 37 °C in a humidified atmosphere containing 5% CO_2. Once at confluence, cells were washed
153 twice with 0.1 mol/L phosphate buffer saline, detached with trypsin-ethylenediaminetetraacetic acid
154 solution, and centrifuged at 270 rfc for 5 min. The pellet was then suspended in complete fresh
155 medium (dilution 1:15) in order to have 1.5×10^4 cells/mL. One milliliter of cell suspension was
156 then seeded in each well of a 24-well plate and incubated at 37 °C in an atmosphere of 5% CO_2.
157 When cells reached 50% of confluence, the culture medium was removed and the test compounds,
158 were added to each well. Cells were incubated with the test compounds for 24 h before cell viability
159 was evaluated through neutral red uptake, using a published procedure (Lamponi, Leone, Consumi,
160 Nelli & Magnani 2020). All samples were set up in six replicates. Complete medium was used as a
161 negative control. The analyses were performed using a UV-VIS Lambda 25 (PerkinElmer
162 Instruments).

163 *Pseudomonas fluorescens (P.F.)* and *Staphylococcus epidermidis (S.E.)* were used to test the
164 influence of Ag silver ions on bacterial proliferation in static conditions. The analysis was
165 conducted following the procedure previously reported (Consumi et al, 2020). Briefly, P.F. and S.E.
166 were inoculated into 5 mL of 30 g/L Tryptic soy broth (TSB) for 24 h at 35.1 °C and RT,
167 respectively. Then, the bacteria stocks were centrifuged for 10 min at 270 rcf, discarding the
168 supernatant. About 5-10 mL of fresh TSB were added to pellets to keep the bacteria alive. Samples

were prepared adding XGP or XGP-AG formulation to bacteria suspension in 1:1 volume ratio. Three replicates for each sample were prepared and their average value was reported. Optical density for Pseudomonas strain at 570 nm (OD 570) and for Staphylococcus at 600 nm (OD 600) were recorded every 30 minutes for 8 h (plateau reached).

3. Results and discussion

3.1 XGP-Ag Complex formation

One of the requirements ophthalmic formulations must meet is a pH value ranging in 6.5–7.6 interval and an osmolality value close to that of human tears, i.e.304 ± 23 mOsm/kg (Craig, Simmons, Patel & Tomlinson, 1995). Phosphorylation, as also observed for other polymers (Leone et al, 2019a), guarantees contemporarily a pH value around 7.1± 0.3 and an osmolality value of 311± 2 mOsm/kg. Moreover, the presence of phosphate groups covalently bound to the XG chains avoids their dispersion in fluid. Indeed, high topical free phosphate ions concentrations can induce corneal calcification. Actually, it is suggested to maintain free phosphate ions concentration close to that of human tears (1.45 mM) (Bernauer, Thiel, Langenauer & Rentsch, 2006). The phosphorylation degree, expressed as P%, resulted 0.01% corresponding to 0.36 % w/w of PO_4^{3-} ions. No phosphate ions release was quantified by XGP and XGP-Ag solutions as a function of time. However, a quantification of the phosphate concentration after possible complete detachment from the chain was simulated and a maximum value of 0.01 mM for the most diluted solution (0.02% w/v) and 0.38 mM for the most concentrated solution (1% w/v) were found. Both the solutions are largely under the critical limit for phosphate ions concentration of 1 mM.

The Ag content from the AAS analysis is 0.33% w/w. No silver ions release was quantified by XGP-Ag solutions as a function of time. However, as done for phosphate ions, a quantification of the silver concentration after possible complete detachment from the chain was simulated and a maximum value of 33 ppm for the most concentrated solution (1% w/v) and 0.7 ppm for the most diluted solution (0.02% w/v) were found. If completely released from the polymer the 1% XGP-Ag

solution could exceed the toxicity limit for silver ions, i.e. 1 ppm (Agarwal et al, 2010; Greulich et al, 2012).

3.3 Infrared Analysis

Infrared spectroscopic measurements were performed to confirm both the phosphorylation of XG polymer and the coordination of silver ions by phosphorylated xanthan gum. IR spectra of native XG, phosphorylated XG (XGP) and metal complex XGP-Ag are depicted in Figure 1. The most evident difference between XG and XGP spectra is the presence of new very intense bands due to phosphate moieties, at 1287 cm^{-1} and at 1016 cm^{-1} (O=P-O stretching and P-O bending, respectively) in XGP spectrum, that confirmed the phosphorylation reaction (Leone et al, 2019a).

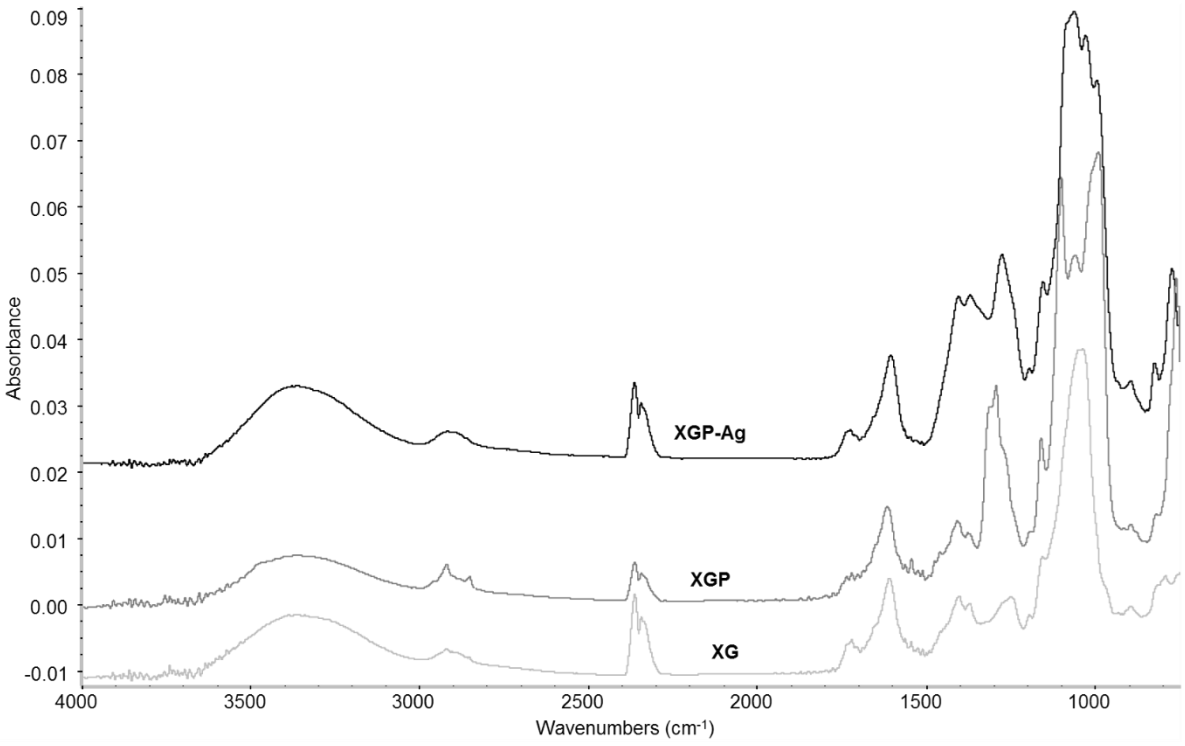

Figure 1: IR spectra of native XG, XGP and XGP-Ag

The coordination mode of silver ions by XGP was highlighted measuring the separation (Δν) between carboxylate asymmetric and symmetric stretching modes. As reported by Fiori-Duarte, de

Paiva, Manzano, Lustri & Corbi (Fiori-Duarte, de Paiva, Manzano, Lustri & Corbi, 2020), a bridged bidentate mode of the COO− group is expected when Δν of the carboxylate group in a metal complex is similar to the Δν of the ligand, whereas a monodentate coordination mode by the carboxylate group is supposed when the Δν of the complex is greater than the ligand. The enlargement of the 1800-1200 cm^{-1} region is depicted in Figure 2 and permits to accurately measure Δν.

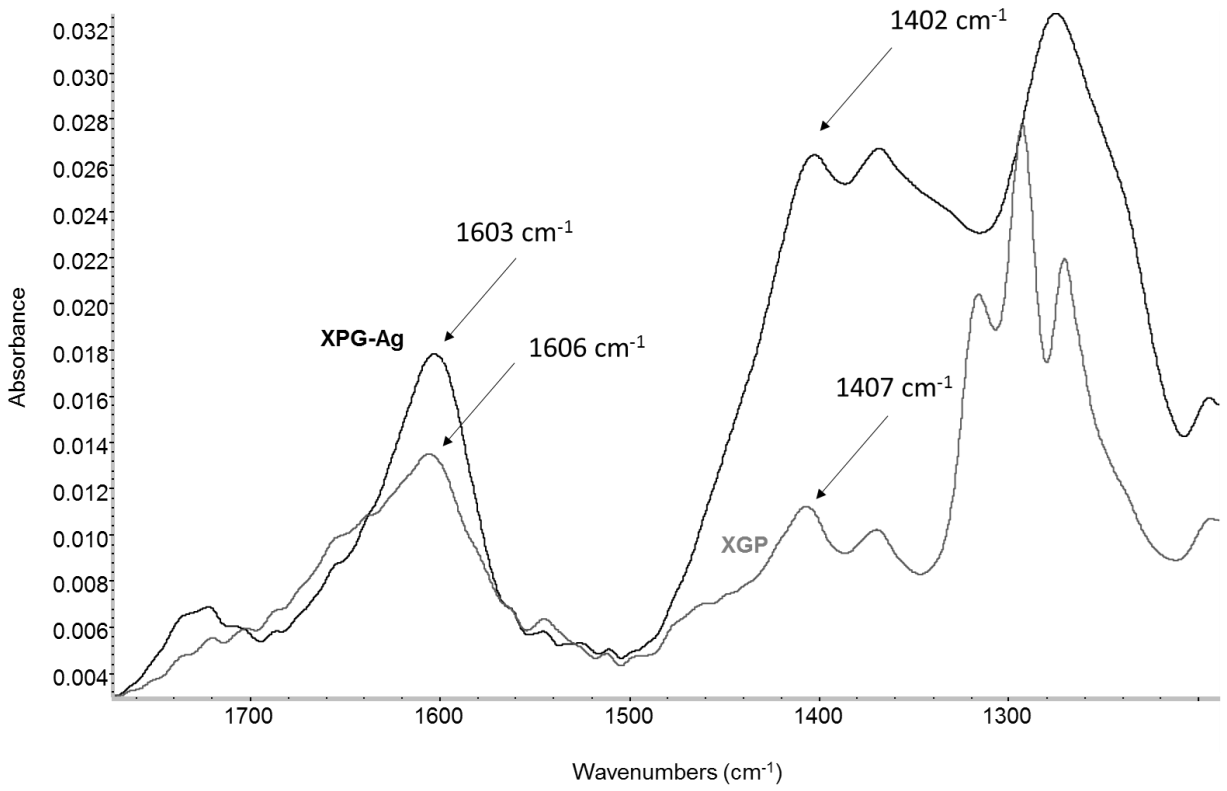

Figure 2: Magnification of the 1800–1200 cm^{-1} region of the spectra, where it is possible to appreciate the shift of carboxylate asymmetric and symmetric stretching bands.

Accordingly with the coordination mode already observed by Fiori-Duarte et al. (Fiori-Duarte et al, 2020) in their sulfasalazine –Ag(I) complex, a bidentate model is found for XGP-Ag. Indeed, a Δν of 199 cm^{-1} was found for XGP polymer whereas a superimposable Δν of 201 cm^{-1} was measured in XGP-Ag. The complex formation can be derived also from the IR bands shape. An enlargement

of the bands suggests a diffuse coordinated system. To confirm this observation TG analysis was also performed.

3.4 Thermal analysis

Thermal behavior of polymeric materials can be analyzed quantifying their weight loss in three different ranges of temperature. The weight loss in 30 °C – 200 °C can be associated with the evaporation of hydration and bulk water, the weight loss in 200 °C-400 °C can be associated to the degradation of free chains whereas the weight loss in 400 °C- 600 °C can be related to the degradation of condensed chains. TG thermographs and relative DTG curves of XG, XGP and XGP-Ag (I) are depicted in Figure 3 and compared to evaluate the effect of phosphorylation and silver ions complexion on thermal behavior of XG. *Per cent* weight losses are summarized in Table 1.

Table 1: Weight loss (mean ± SD; n = 3) of samples in the analyzed ranges, the calculated R-value (ratio between the weight loss in 400-600 °C and 200-400 °C ranges) and the corresponding residue at 600°C.

Sample	30°C-200°C	200°C-400°C	400°C-600°C	R	Residue (600°C)
XG	11% ± 1%	50% ± 2%	7% ± 1%	0.14 ± 0.01	32% ± 2%
XGP	23% ± 1%	33% ± 4%	5% ± 3%	0.15 ± 0.01	38% ± 3%
XGP-Ag	9% ± 1%	40% ± 3%	8% ± 1%	0.20 ± 0.01	42% ± 2%
CegD	10% ± 1%	56% ± 2%	12% ± 1%	0.21 ± 0.01	22% ± 2%

XG: native xanthan gum; XGP: phosphorylated xanthan gum; XGP-Ag: phosphorylated xanthan gum–Ag(I) complex; CegD: Commercial eye gel Drops

240 The insertion of hydrophilic phosphate groups along the chain increased the water binding capacity
241 of native XG, doubling the weight loss in the first range of temperature. The coordination of silver
242 ions decreased the water holding capacity. Indeed, XGP-Ag showed a water binding capacity
243 significantly lower than both native and phosphorylated polymers. Ag(I) complexion significantly
244 affects the water binding capacity of phosphorylated polymer both shielding the negatively charged
245 moieties and reducing the free motion of polymer chains. This compaction of the system can be
246 confirmed calculating R, that is the ratio between the weight loss in the 400-600 °C temperature
247 range and the weight loss in the 200-400 °C temperature range. It is associated to the degree of
248 structuration of the material (Leone et al, 2019 c). R increases from 0.15 to 0.20 in the presence of
249 Ag(I) ions. The Ag (I) complexion stabilizes the system as also highlighted by the significant
250 increase of the temperature at which the highest weight loss is observed (XGP: 292 °C *vs* 303 °C
251 for XGP-Ag) (Figure 3B). Interestingly, comparing XGP and XGP-Ag thermographs we can
252 observe the separation of the main weight loss band of XGP into two portions. The one centered at
253 a higher temperature (303 °C) can be associated to the degradation of chains involved in Ag (I)
254 complexion whereas the one centered at a lower temperature (223 °C) can be associated to the
255 degradation of free chains not involved in metal ions coordination. The last one falls at a lower
256 temperature in comparison with native XGP chains (292 °C) for the disruption of the homogeneity
257 of the system and the rupture of diffused hydrogen bonds between hydrophilic groups. Indeed, as
258 highlighted by the weight loss percentages, the presence of phosphate moieties along the chains
259 significantly increases the water binding capacity of the polymer and, consequently, increases the
260 hydrogen bonds network that stabilizes the polymeric system (XG: 276 °C *vs* XGP: 292 °C).
261 Finally, as expected, any treatment, i.e. phosphorylation and addition of silver ions, increased the
262 relative amount of the residue that passes from 32% to 38% and to 42% for the metal complex.

263 Thermal behavior of the commercial eye gel drop formulation was also analyzed and its weight loss
264 reported in Table 1. TG thermograph and the relative DTG curve of CegD are depicted in Figure

3C. Even if from a qualitative point of view the two systems, i.e. XGP-Ag and CegD cannot be compared being based on different polymers (xanthan gum and a mixture of PEG and hydroxyguar, respectively), nevertheless, a similar thermal behaviour can be observed. In particular, the presence of silver ions induces a similar stabilization to that observed for the gel based formulation having a similar R value (Table 1).

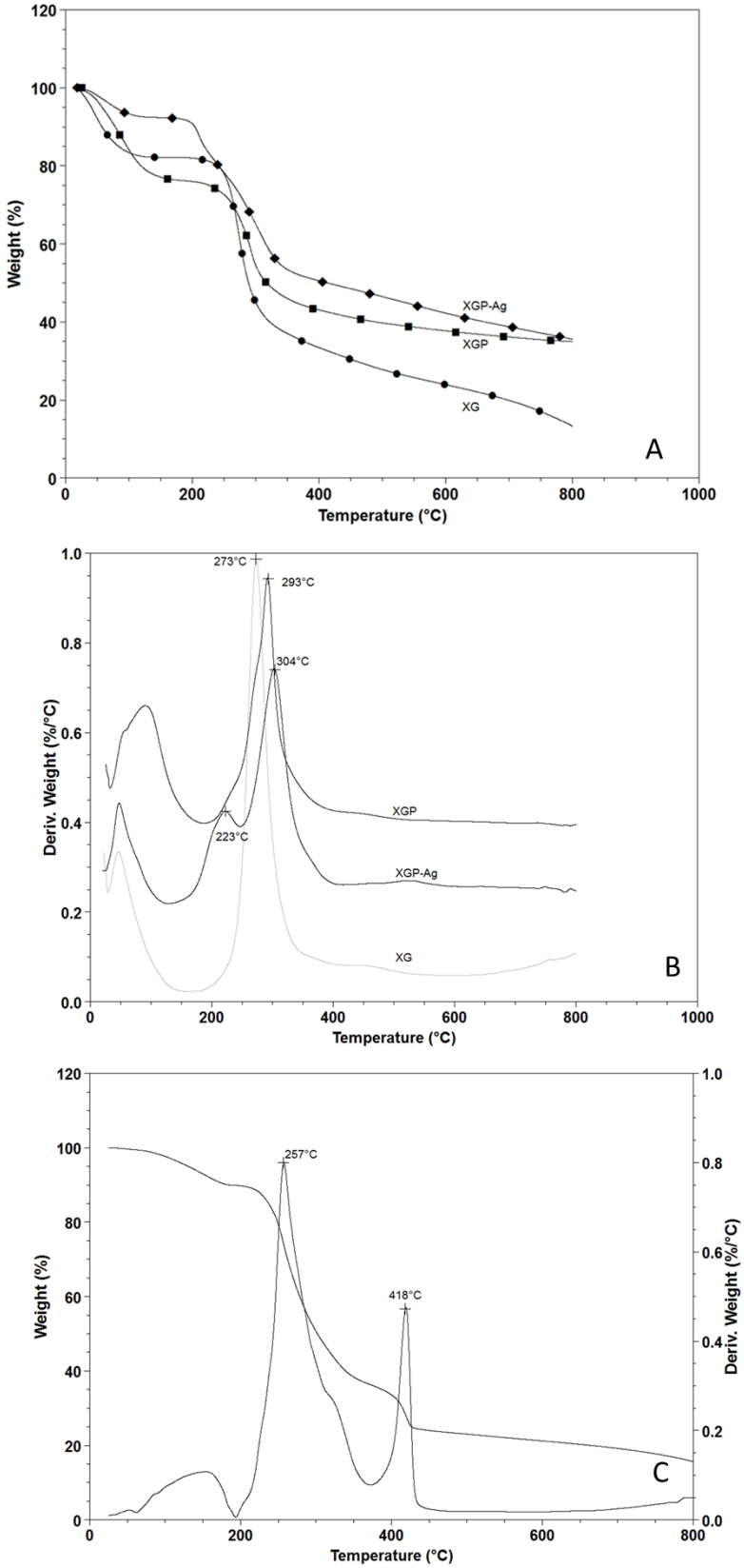

Figure 3: A: weight (%) *versus* temperature in 30-800 °C for XG, XGP and XGP-Ag samples; B: derivative of weight *versus* temperature in 30-800 °C for XG, XGP and XGP-Ag samples; C: TG and DTG curves of a commercial eye gel drop formulation (CegD).

3.5 Rheology

To insight the effect of phosphorylation and silver ions on rheological performance of xanthan gum, mechanical spectra of XG 1% w/v, XGP 1% w/v and XGP-Ag 1% w/v solutions were recorded and compared. Results are reported as complex shear modulus (G* = G'+iG") (Figure 4A) and tan δ (tan δ = G"/G') (Figure 4B), where G" and G' are respectively the loss and storage modulus.

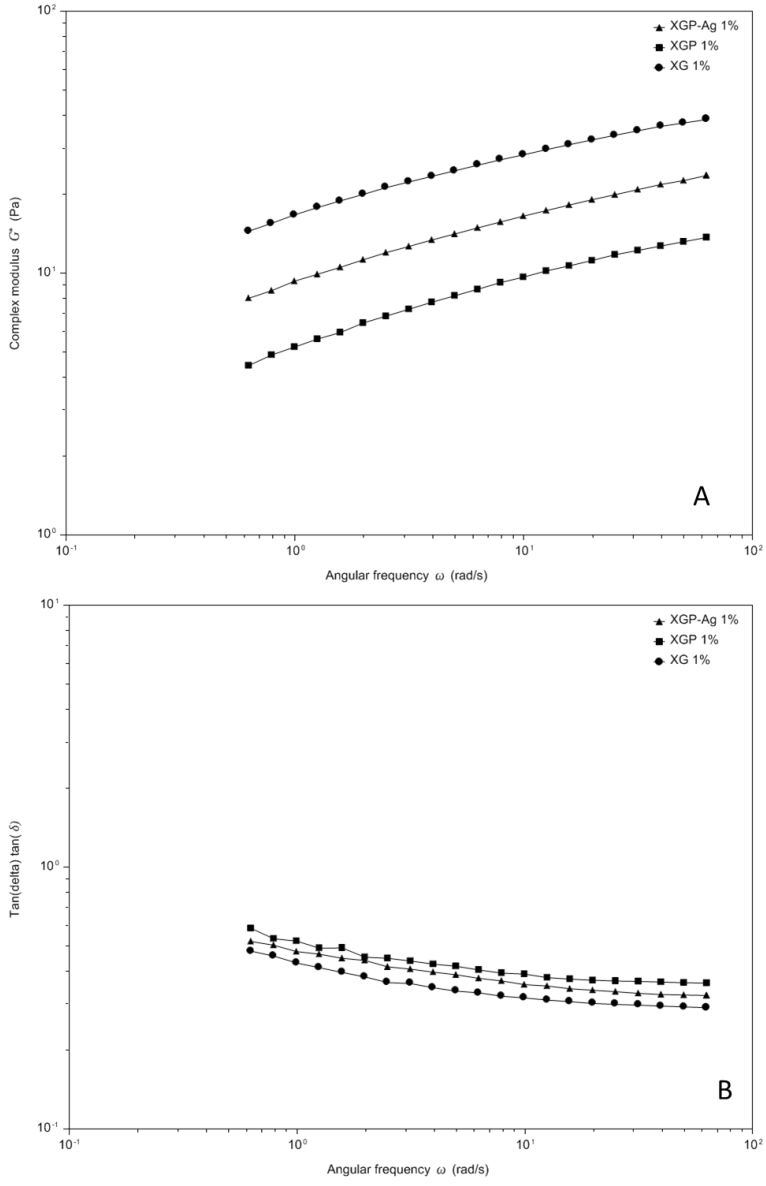

Figure 4: A: A: Complex modulus G* as a function of angular frequency for 1% w/v solution of XG (●), XGP (■) and XGP-Ag (▲); B: Tan δ as a function of angular frequency for 1% w/v solution of XG (●), XGP (■) and XGP-Ag (▲)

G* gives information on the overall mechanical properties of the product that is subjected to a shear strain. The tan δ parameter gives information about the relative contribution of G' and G" on the overall mechanical properties. In accordance with the observations derived from thermal analysis, the presence of phosphate moieties along the chains strongly affects XG properties. XGP high water-binding capacity is reflected in a general decrease of mechanical performance. The subsequent addition of silver ions reduced the effect of phosphate moieties on the mechanical properties thank to the compaction of the structure moving the overall mechanical performance of the formulation close to that of a widely used commercial product. The slope of G* curves for XG, XGP and XGP-Ag is quite the same ranging from 0.17 for XG to 0.26 for XGP-Ag. Tan δ, the ratio between the two moduli, permits to evaluate the predominance of the dissipative or conservative contribution to the performance, or, in other words, when the viscous or elastic behavior is predominant. Tan δ is 1 when G" = G' and corresponds to the crossover point (COP). The presence of silver ions significantly stabilizes the system whose tan δ is always under 1 or the elastic component predominates on its viscous component, differently from what observed for XGP solution. A tan δ value lower than 1 is not a limiting parameter for the foreseen application. Indeed, actually several gel based vehicles have been developed to be used as eye drops (Chen et al, 2021; Luo, Nguyen & Lai, 2020; Shelley, Rodriguez-Galarza, Duran, Abarca & Babu, 2018). Nevertheless, three different concentrations of XGP-Ag were tested to find the formulation showing the best performance for the foreseen application as eye drop. 0.02% w/v, 0.5% w/v and 1.0% w/v solutions of XGP-Ag were prepared. Before performing any rheological analyses, all the prepared formulations were sterilized by filtration (through 0.22 µm filter) that is more convenient and effective than an aseptic production process especially for liquid not particulate formulations, as also highlighted by Imperiale et al. (Imperiale et al, 2018). The effect of subsequent filtration steps was evaluated recording viscosity curves. A significant effect was observed only for the first filtration step that provokes a viscosity decrease at low shear rate values from 20 % for 0.02%

309 formulation to 50% for 0.5% formulation. The further filtration step did not affect significantly
310 formulations viscosity ($p<0.05$) (Figure S1).

311 Storage and loss moduli of XGP-Ag 0.02%, 0.5% and 1% after the first filtration step (F1) as a
312 function of oscillation frequency were measured and compared with the commercial product to
313 select the best concentration for the foreseen application. In Figure 5A complex moduli were
314 depicted to get information on the overall mechanical properties of the products. Different slopes
315 were obtained thus highlighting a different dependence from the oscillation. XGP-Ag 1%
316 mechanical performance showed a very low dependence from the oscillation thus highlighting its
317 stability but at the same this behavior could limit its applicability as eye drops. On the contrary,
318 both XGP-Ag 0.5% and XGP-Ag 0.02% showed a slope, or a dependence from oscillation, close to
319 that of commercial product. G' and G" were shown in Figure 5B.

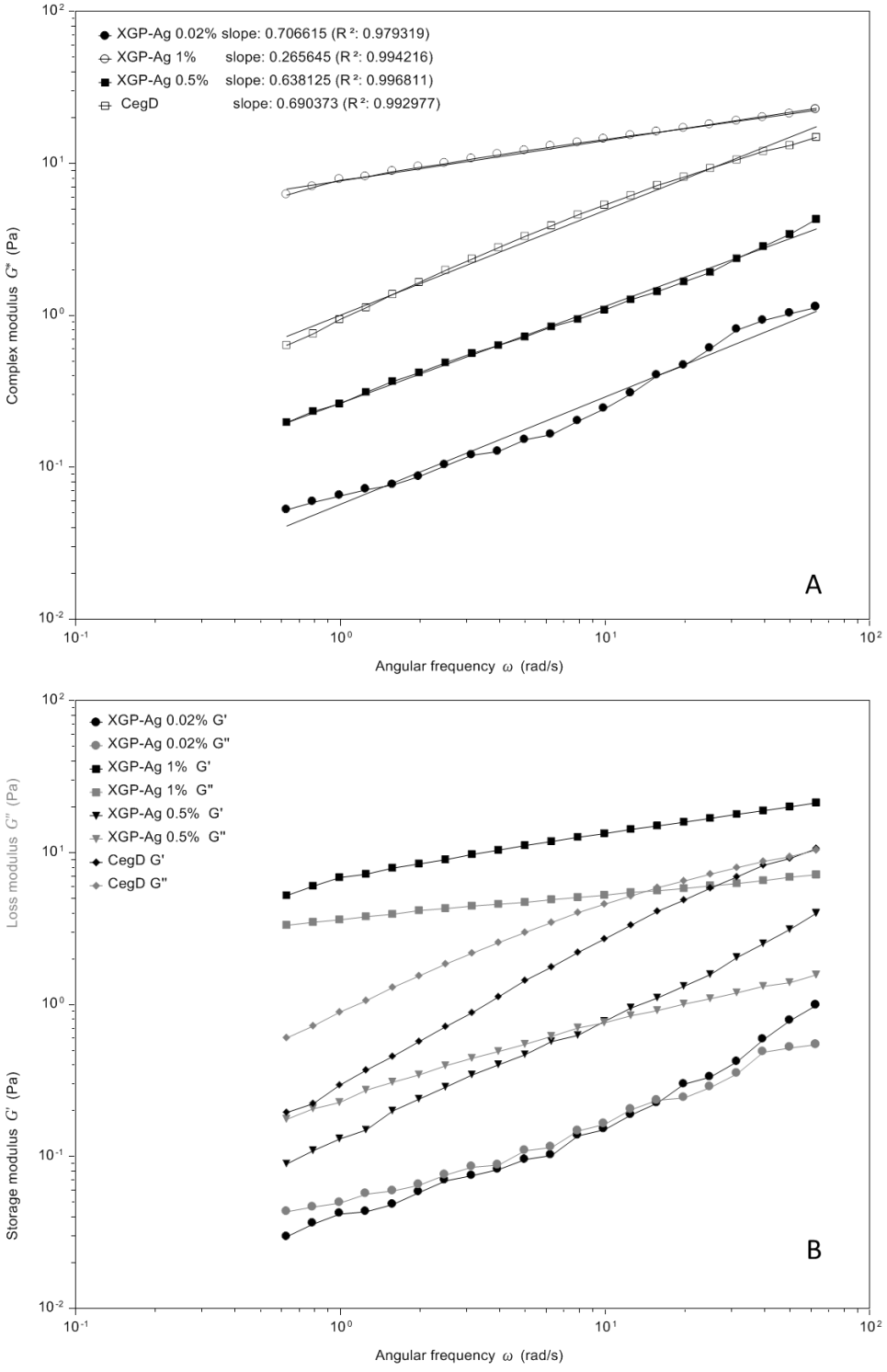

320

321 **Figure 5: A:** Complex modulus G* as a function of angular frequency of XGP-Ag 1%, XGP-Ag

322 0.5%, XGP-Ag 0.02% and CegD; B: G' and G" as a function of angular frequency of XGP-Ag 1%,

323 XGP-Ag 0.5%, XGP-Ag 0.02% and CegD.

324

XGP-Ag 0.02% and XGP-Ag 0.5 % both showed a crossover point as well as the commercial product even if at lower frequency values. To confirm their applicability for the foreseen application the viscosity behavior was analyzed. Indeed, adequate viscosity is the most important requirement for eye drops.

The viscosity curves of all the solutions after the first filtration step (F1) were recorded and compared with the viscosity curve of the commercial eye gel-drops (CegD) (Figure 6).

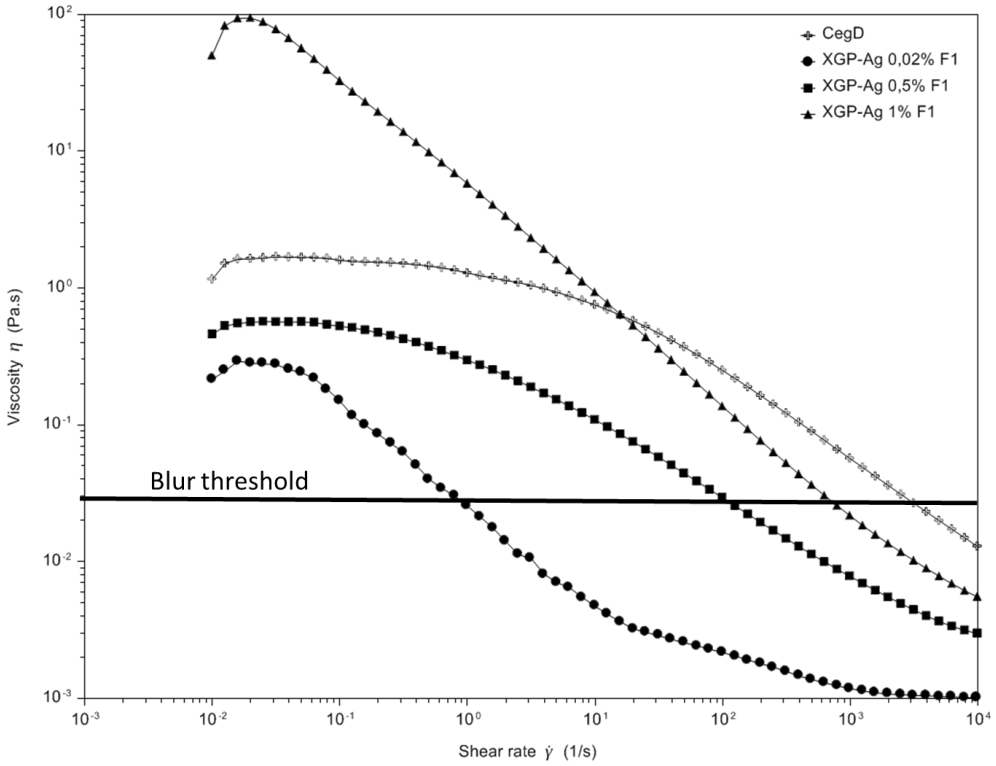

Figure 6: Viscosity curve of 1%, 0.5% and 0.02% aqueous solutions of XGP-Ag after first filtration step and a commercial gel eye drops product (CegD)

All the tested solutions show a typical shear-thinning behavior with viscosity that decreases as a function of shear rate. Since human tears are considered a Newtonian fluid, in the past also for eye drops this behavior was preferred. Actually, a shear-thinning behavior is preferred since during the interblink period shear-thinning solutions act as high viscous fluids leading to reduced drainage

rates and prolonged residence time (Zhu & Chauhan, 2008). On the contrary, during blinking, when a very high shear rate is present, pseudo-plastic solutions exhibit very low viscosity and drainage does not induce any discomfort for the patient. Eye drops should be not only more viscous than human tears (1.5 mPa·s) (Zhu & Chauhan, 2008) but also reach a viscosity value close to 10 mPa·s, since the retention began to increase only after the fluid viscosity exceeded that critical value (Zaki, Fitzgerald, Hardy & Wilson, 1986). Contemporarily, viscosity should not exceed the threshold value of 30 mPa.s to avoid any sticking sensation. Different shear rate values were proposed for both the interblinking and the blinking phase (Aragona, Simmons, Wang & Wangwere, 2019; Müller-Lierheim 2020; Račić et al, 2019). Despite the specific considered values for both the phases, it is of outmost importance that during interblinking phase eye drops formulations reach 10 mPa.s value to assure retention and during blinking phase do not exceed 30 mPa.s to avoid sticky sensation (blur threshold). All viscosity curves were analyzed selecting the best fit flow (viscosity *vs* rate), that resulted Cross model, to obtain the zero shear viscosity (XGP-Ag 1.0% w/v: η_0= 77600±987 mPa.s, R^2 0.999; XGP-Ag 0.5% w/v: η_0 = 609±39, R^2 0.999; XGP-Ag 0.02% w/v: η_0 = 495±15, R^2 0.995; CegD: η_0 = 1620±56, R^2 0.999). Among the tested formulations XGP-Ag 0.02% reaches the blur threshold at very low shear rate (γ 1 s^{-1}) thus resulting the most promising solution.

3.6 Transparency and Refractive Index

Another fundamental parameter for eye drops is a refractive index of about 1.35±0.01 (Imperiale et al, 2018) or transparency index higher than 85%, considering their low residence time. All the sterilized formulations were analyzed to evaluate their transparency in the visible range 380 nm - 700 nm and all the samples guaranteed a visible light transmission higher than 85% (Figure 7).

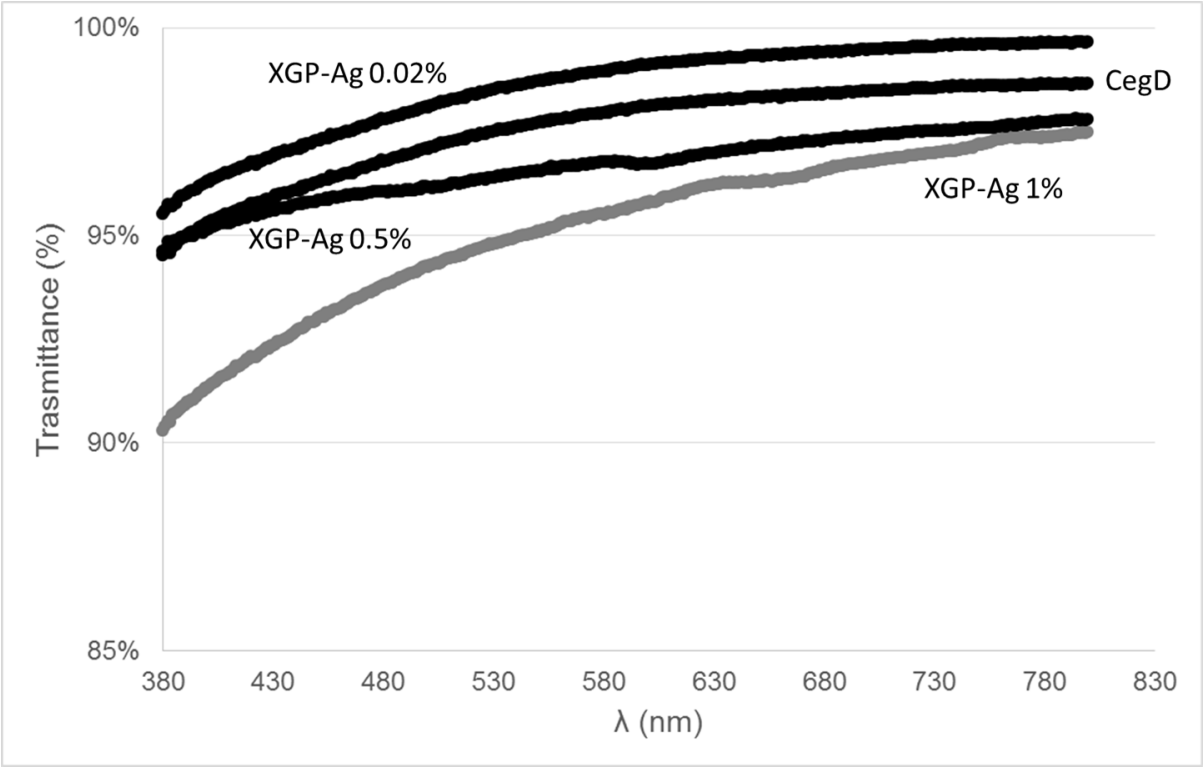

Figure 7: Light Trasmittance (%) along visible spectrum of XGP-Ag 0.05%, XGP-Ag 0.02% and XGP-Ag 1% solutions.

Despite all formulations can be defined as transparent ones, nevertheless XGP-Ag 1% shows a lower optical transparency in the range of 380-550 nm (values: 0.903±0.01- 0.951±0.02) that does not avoid its applicability for the foreseen application. No significant differences ($p<0.05$) were found for XGP-Ag 0.02% (values: 0.955±0.02 - 0.987±0.01), XGP-Ag 0.5% (values: 0.946±0.01 - 0.966±0.01) and CegD (values: 0.945±0.01 - 0.977±0.01) in the 380-550 nm range.

No significant differences ($p<0.05$) were found in terms of refractive index for all the tested formulation. In particular, a refractive index of 1.33±0.01 was found for XGP-Ag 0.02% and XGP-Ag 0.5% and a superimposable value of 1.34±0.01 for XGP-Ag 1% and CegD.

3.7 Biological characterization

375 Cytotoxicity of increasing concentrations of XGP and XGP-Ag formulations and of CegD was
376 assessed using NIH3T3 and HMVEC cells. HMVEC cells were selected basing on the high
377 vascularization of the eye. All XGP solutions as well as the commercial product (CegD) did not
378 show any toxic effect towards both NHI3T3 and HMVEC cells whereas in the presence of silver
379 ions different behaviors were observed. The most diluted formulation did not show any toxic effect
380 on both NIH3T3 and HMVEC proliferation. Increasing the concentration of 25 times (from 0.02%
381 to 0.5%) an increase of 10% of toxicity is observed towards NIH3T3 and an increase of 13% of
382 toxicity towards HMVEC. Doubling the concentration of XGP-Ag (XGP-Ag 1%) a further increase
383 in cytotoxicity of 8% and 20% towards NIH3T3 and HMVEC, respectively was recorded. (Figure
384 8A).

385 The commercial product contains polyquaternum-1, a BAC derivative able to hinder bacterial
386 proliferation. The capability of the most diluted formulation to similarly hinder bacterial
387 proliferation was verified. Two available bacterial strains, i.e. *Pseudomans fluorescens* and
388 *Staphylococcus epidermidis* were used. As shown in Figure 8B and 8C, the addition of
389 phosphorylated polysaccharide to bacterial medium (TBS) strongly stimulate bacterial proliferation
390 that is particularly evident for *Pseudomonas fluorescens*. Contrarily, the addition of XGP-Ag
391 formulation to TBS hinders bacterial proliferation, of about 50% showing a comparable behavior to
392 in comparison to phosphorylated polymer and about 30% in comparison with pure TSB. The
393 measurements were stopped after 8h being reached the plateau.

394

395

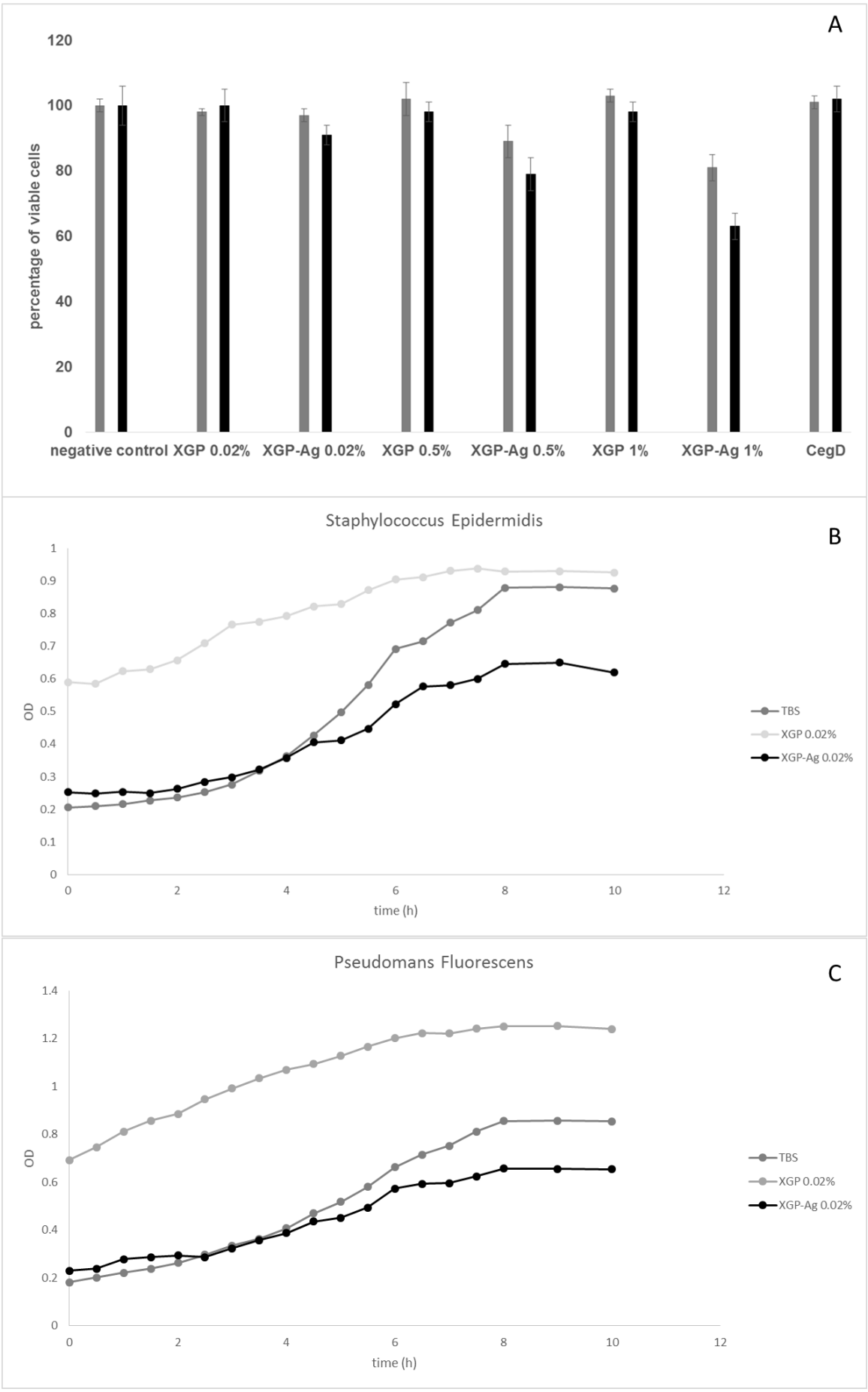
A
120
100
80
60
40
20
0
percentage of viable cells
negative control
XGP 0.02%
XGP-Ag 0.02%
XGP 0.5%
XGP-Ag 0.5%
XGP 1%
XGP-Ag 1%
CegD
B
Staphylococcus Epidermidis
OD
time (h)
TBS
XGP 0.02%
XGP-Ag 0.02%
C
Pseudomans Fluorescens
OD
time (h)
TBS
XGP 0.02%
XGP-Ag 0.02%

396

Figure 8: A: Percentage of viable fibroblasts NIH3T3 and HMVEC evaluated by the neutral red assay. Data are means ± SD of experiments run in triplicate. Only the negative control (LDPE) is reported. The positive control (organo-tin-stabilized polyurethane) has not been reported because the percentage of viable cells is 0%; **B:** Proliferation of *Staphylococcus epidermidis* as a function of time; **C**: Proliferation of *Pseudomonas fluorescens* as a function of time.

Conclusions

Xanthan Gum was phosphorylated using sodium trimetaphosphate. The modified polymer was enriched with silver ions. Infrared and thermal analysis confirmed both the phosphorylation and the metal ions complexion. 1%, 0.5% and 0.02% w/v solutions were tested to verify the accomplishment of eye drops formulation requirements, i.e., pH, osmolality, transparency, viscosity and sterility. All the analyzed solutions showed pH, osmolality and transparency values close to that of human tears. Nevertheless, the most concentrated solution (1% XGP-Ag) resulted to viscous for the foreseen application. Cytotoxicity analysis confirmed the good performance of the most diluted solution (XGP-Ag 0.02%) that was able to hinder bacterial proliferation, despite the low amount of silver ions. The obtained results let us to conjecture that XGP-Ag (I) could be used as viscosity enhancer for eye drops.

Data availability

Upon request to corresponding author.

Declaration of Competing Interest

None.

Acknowledgement

This research did not receive any specific grant from funding agencies in the public, commercial, or not-for-profit sectors. Authors would like to thank INSTM for support.

References

Agarwal, A., Weis, T. L., Schurr, M. J., Faith, N. G., Czuprynski, C. J., McAnulty, J. F., Murphy, C.J., & Abbott, N. L. (2010). Surfaces modified with nanometer-thick silver-impregnated polymeric films that kill bacteria but support growth of mammalian cells. *Biomaterials*, 31, 680-690.

Aragona, P., Simmons, P.A., Wang, H., and Wangwere, T. (2019). Physicochemical Properties of Hyaluronic Acid–Based Lubricant Eye Drops. Translational Vision Science & Technology, 8 (6), 2.

Bernauer, W., Thiel, M.A., Langenauer, U.M., & Rentsch, K.M. (2006). Phosphate concentration in artificial t ceears, *Graefe's Archive for Clinical and Experimental Ophthalmology,* 244, 1010–1014.

Bonilla-Gameros, L., Chevallier, P., Sarkissian, A., & Mantovani, D. (2020). Silver-based antibacterial strategies for healthcare-associated infections: Processes, challenges, and regulations. An integrated review. *Nanomedicine: Nanotechnology, Biology and Medicine*, 24, 102142.

Cappelli, A., Paolino, M., Grisci, G., Razzano, V., Giuliani, G., Donati, A., Bonechi, C., Mendichi, R., Battiato, S., Samperi, F., Scialabba, C., Giammona, G., Makovec, F., Licciardi M. (2016). Hyaluronan-coated polybenzofulvene brushes as biomimetic materials. *Polymer Chemistry*, 7, 6529-6544.

Chen, Z., Yang, M., Wang, Q., Bai, J., McAlinden, E., Skiadaresi, E., Zhang, J., Pan, L., Mei, C., Zeng, Z., Yu, J., Feng, Y., Jiang, Z., fXu, W., Xu, H., Ye, X., He, H., Wang, Q., Deng, J., Huang, J. (2021).Hydrogel eye drops as a non-invasive drug carrier for topical enhanced

444 Adalimumab permeation and highly efficient uveitis treatment. *Carbohydrate Polymers,* 253,
445 117216

446 Consumi, M., Jankowska, K., Leone, G., Rossi, C:, Pardini, A., Robles, E., Wright, K., Brooker,
447 A., & Magnani A. (2020). Non-destructive monitoring of p. Fluorescens and s. epidermidis
448 biofilm under different media by fourier transform infrared spectroscopy and other
449 corroborative techniques. *Coatings*, 10, 930.

450 Craig, J.P., Simmons, P.A., Patel, S., Tomlinson, A. (1995). Refractive index and osmolality of
451 human tears, *Optometry and Vision Science*, 72, 718–724.

452 Dzionek, A., Wojcieszyńska, D., Adamczyk-Habrajska, M., Karczewski, J., Potocka, I. &
453 Guzik, U. (2021). Xanthan gum as a carrier for bacterial cell entrapment: Developing a novel
454 immobilised biocatalyst. *Materials Science and Engineering: C*, 118, 111474.

455 Fiori-Duarte, A.T., de Paiva, R.E.F., Manzano, C.M., Lustri, W.R., & Corbi, P.P. (2020). Silver
456 (I) and gold (I) complexes with sulfasalazine: Spectroscopic characterization, theoretical studies
457 and antiproliferative activities over Gram-positive and Gram-negative bacterial strains. *Journal*
458 *of Molecular Structure*, 1214, 128158.

459 Greulich, C., Braun, D., Peetsch, A., Diendorf, J., Siebers, B., Epple, M., & Köller, M. (2012).
460 The toxic effect of silver ions and silver nanoparticles towards bacteria and human cells occurs
461 in the same concentration range. *RSC Advances*, 2, 6981-6987.

462 Imperiale, J.C., Gabriela B. Acosta, G.B., Alejandro Sosnik, A. (2018). Polymer-based carriers
463 for ophthalmic drug delivery. *Journal of Controlled Release,* 285, 106-141.

464 Jumelle, C., Gholizadeh, S., Annabi, S. & Dana, R. (2020). Advances and limitations of drug
465 delivery systems formulated as eye drops, *Journal of Drug Delivery Science and Technology*,
466 321, 1-22.

Karakus, S., Ilgar, M., Tan, E., Kahyaoglu, I.M., Tasaltin, N., Albayrak, I., Insel, M.A., Kilislioglu, A. (2020). Preparation and characterization of carboxymethyl cellulose/poly (ethyleneglycol) -rosin pentaerythritolester polymeric nanoparticles: Role of intrinsic viscosity and surface morphology. *Surfaces and Interfaces*, 21, 100642.

Lamponi, S., Leone, G., Consumi, M., Nelli N., Magnani, A.(2020). Porous multi-layered composite hydrogel as cell substrate for in vitro culture of chondrocytes, *International Journal of Polymeric Materials and Polymeric Biomaterials*, DOI: 10.1080/00914037.2020.1765351

Leone, G., Consumi, M., Pepi, S., Lamponi, S., Bonechi, C., Tamasi, G., Donati, A., Rossi, C., Magnani, A. (2017). Alginate-gelatin formulation to modify lovastatin release profile from red yeast rice for hypercholesterolemia therapy. *Therapeutic Delivery*, 8, 843–854.

Leone, G., Consumi, M., Pepi, S., Pardini, A., Bonechi, C., Tamasi, G., Donati, A., Rossi, C., & Magnani, A. (2019 a). Modified low molecular weight poly-vinyl alcohol as viscosity enhancer. *Materials Today Communications*, 21, 100634.

Leone, G., Consumi, M., Lamponi, S., Bonechi, C., Tamasi, G., Donati, A., Rossi, C. & Magnani, A. (2019 b). Hybrid PVA-xanthan gum hydrogels as nucleus pulposus substitutes. *International Journal of Polymeric Materials and Polymeric Biomaterials*, 68, 681-690.

Leone, G., Consumi, M., Lamponi, S., Bonechi, C., Tamasi, G., Donati, A., Rossi, C., Magnani, A. (2019 c). Thixotropic PVA hydrogel enclosing a hydrophilic PVP core as nucleus pulposus substitute. *Materials Science and Engineering C*, 98, 696–704.

Leone, G., Consumi, M., Pepi, S., Pardini, A., Bonechi, C., Tamasi, G., Donati, A., Lamponi, S., Rossi, C., Magnani, A. (2020). Enriched Gellan Gum hydrogel as visco-supplement, *Carbohydrate Polymers*, 227, 115347.

489 Lin, C.H., Lin, W.C., Yang, M.C. (2009). Fabrication and characterization of ophthalmically
490 compatible hydrogels composed of poly(dimethyl siloxane-urethane)/Pluronic F127. *Colloids*
491 *and Surface B Biointerfaces*, 71, 36–44.

492 Ludwig, A. (2005). The use of mucoadhesive polymers in ocular drug delivery. *Advanced Drug*
493 *Delivery Reviews,* 57, 1595–1639.

494 Luo, L.J., Nguyen, D.D. Lai, J.Y. (2020). Long-acting mucoadhesive thermogels for improving
495 topical treatments of dry eye disease. *Materials Science and Engineering: C*, 115, 111095.

496 Mahboobian, M.M., Mohammadi, M., Mansouri, Z. (2020). Development of thermosensitive in
497 situ gel nanoemulsions for ocular delivery of acyclovir. *Journal of Drug Delivery Science and*
498 *Technology,* 55, 101400

499 Müller-Lierheim W.G.K. (2020).Why Chain Length of Hyaluronan in Eye Drops Matters?
500 Diagnostics, 10, 511.

501 Piluso, P., Sudre, G., Boisson-Da Cruz, F., Bounor-Legaré, V., Espuche, E. (2018). Impact of
502 10-undecenal PVA acetalization on the macromolecular organization and the viscosity of
503 aqueous solutions. Surface and bulk properties of the modified PVA films. *European Polymer*
504 *Journal*, 108, 412-419.

505 Račić, A., Čalija, B., Milić, J., Milašinović, N. & Krajišnik, D. (2019). Development of
506 polysaccharide-based mucoadhesive ophthalmic lubricating vehicles: The effect of different
507 polymers on physicochemical properties and functionality, *Journal of Drug Delivery Science*
508 *and Technology*, 49, 50-57.

509 Rinaudo, M. (2008). Main properties and current applications of some polysaccharides as
510 biomaterials. *Polymer International*, 57, 397–430, 2008.

511 Said dos Santos, R., Rosseto, H.C., Bassi da Silva, J., Félix Vecchi, C., Caetano, W., Bruschi,
512 M.L. (2020).The effect of carbomer 934P and different vegetable oils on physical stability,
513 mechanical and rheological properties of emulsion-based systems containing propolis. *Journal*
514 *of Molecular Liquids*, 307, 112969.

515 Salzillo, R., Schiraldi, C., Corsuto, L., D'Agostino, A., Filosa, R., De Rosa, M., La Gatta, A.
516 (2016). Optimization of hyaluronan-based eye drop formulations. *Carbohydrate Polymers*, 153,
517 275–283.

518 Shelley, H., Rodriguez-Galarza, M.R., Duran, S.H., Abarca, E.M., Babu R.J. (2018).In Situ Gel
519 Formulation for Enhanced Ocular Delivery of Nepafenac. *Journal of Pharmaceutical Sciences*,
520 107, 3089-3097.

521 Waszczykowska, A., Żyro, D., Jurowski, P. Ochocki, J. (2020). Effect of treatment with
522 silver(I) complex of metronidazole on ocular rosacea: Design and formulation of new silver
523 drug with potent antimicrobial activity. *Journal of Trace Elements in Medicine and Biology*, 61,
524 126531

525 Wroblewska, K., Kucinska, M., Murias, M. & Lulek, J. (2015). Characterization of new eye
526 drops with choline salicylate and assessment of their irritancy by in vitro short time exposure
527 tests. Saudi Pharmaceutical Journal, 23, 407-412.

528 Zhang, R., Park, M., Richardson, A., Tedla, N., Pandzic, E., de Paiva, C.S., Watson, S.,
529 Wakefield, D. & Di Girolamo, N.(2020). Dose-dependent benzalkonium chloride toxicity
530 imparts ocular surface epithelial changes with features of dry eye disease. *The Ocular Surface,*
531 18, 158-169.

532 Zhu, H. & Chauhan, A. (2008). Effect of Viscosity on Tear Drainage and Ocular Residence
533 Time. *Optometry and Vision Science*, 85, E715-E725

534 Zaki, I., P. Fitzgerald, P., Hardy, J.G., Wilson, C.G. (1986). A comparison of the effect of
535 viscosity on the precorneal residence of solutions in rabbit and man. *Journal of Pharmacy and*
536 *Pharmacology*, 38, 463-466.

537